Available online at www.sciencedirect.com
SCIENCE DIRECT
Tetrahedron
Tetrahedron 62 (2006) 6981–6989

New antitumor sesquiterpenoids from *Santalum album* of Indian origin

Tae Hoon Kim,[a] Hideyuki Ito,[a,*] Tsutomu Hatano,[a] Junko Takayasu,[b] Harukuni Tokuda,[b] Hoyoku Nishino,[b] Takahisa Machiguchi[c] and Takashi Yoshida[d]

[a]*Pharmaceutical Sciences, Okayama University Graduate School of Medicine, Dentistry and Pharmaceutical Sciences, Tsushima, Okayama 700-8530, Japan*
[b]*Department of Molecular Biochemistry, Kyoto Prefectural University of Medicine, Kamigyo-ku, Kyoto 602-0842, Japan*
[c]*Faculty of Science, Saitama University, Sakura-ku, Saitama 338-8570, Japan*
[d]*Faculty of Pharmaceutical Sciences, Matsuyama University, Bunkyo-chou, Matsuyama, 790-8578, Japan*

Received 10 March 2006; revised 20 April 2006; accepted 21 April 2006
Available online 30 May 2006

Abstract—Three new campherenane-type (**1**, **4**, **7**) and three new santalane-type (**9**, **11**, **12**) sesquiterpenoids, and two aromatic glycosides (**21**, **22**) together with 12 known metabolites including α,β-santalols (**14**, **18**), (*E*)-α,β-santalals (**15**, **19**), α,β-santaldiols (**16**, **20**), α-santalenoic acid (**17**), and vanillic acid 4-*O*-neohesperidoside were isolated from *Santalum album* chips of Indian origin. The structures of the new compounds, including absolute configurations, were elucidated by 1D- and 2D-NMR spectroscopic and chemical methods. The antitumor promoting activity of these isolates along with several neolignans previously isolated from the same source was evaluated for both in vitro Epstein–Barr virus early antigen (EBV-EA) activation and in vivo two-stage carcinogenesis assays. Among them, compound **1** exhibited a potent inhibitory effect on EBV-EA activation, and also strongly suppressed two-stage carcinogenesis on mouse skin.

1. Introduction

The plants belonging to the genus *Santalum* (Santalaceae), which are evergreen parasitic trees and consist of about 25 species, are distributed throughout India, Indonesia, Malaysia, and Australia.[1] Their essential oil (sandalwood oil) is widely used in the cosmetic, perfumery, and aromatherapy industries and has been reported to have various biological properties such as antiviral,[2] anticarcinogenesis,[3] and antitumor effects.[4,5] Among the reported constituents including sesquiterpenoids, triterpenoids,[6–11] and phenylpropanoids,[12] α-santalol, which is one of the major components in most species of the *Santalum* genus, is responsible for most of the activity of the oil. α-Santalol has particularly attracted increasing attention for its neuroleptic property[13–15] and chemopreventive effect[16–17] in in vitro and in vivo bioassay systems. In our continuing study on minor constituents of the heartwood of Indian *S. album*, grown in the Mysore district, which is known as the best tree producing sandalwood,[18] we reported the isolation and characterization of new neolignans[19] and bisabolol-related sesquiterpenoids.[20] Upon further investigation of the same plant, we have isolated and characterized six new sesquiterpenoids and two new phenolic glycosides, together with 12 known compounds that were structurally related to campherenane and santalane skeletons. We report herein the isolation and structure elucidation of the new compounds, and their inhibitory effect on EBV-EA activation in Raji cells, which is used as a convenient in vitro assay for assessing antitumor promoting activity. In vivo antitumor promoting activity was also evaluated by two-stage mouse skin carcinogenesis test.

2. Results and discussion

A methanol extract of chopped heartwood of *S. album* was divided into *n*-hexane-, ethyl acetate-, and water-soluble portions by solvent partition. The combination of chromatographic separation of the *n*-hexane, ethyl acetate, and water-soluble extracts gave eight new compounds (**1**, **4**, **7**, **9**, **11**, **12**, **21**, and **22**) and 12 known metabolites, 2α,12-dihydroxy-10(*Z*)-campherene (**2**),[21] 2β,12-dihydroxy-10(*Z*)-campherene (**5**),[21] 10(*Z*)-sandalnol (**10**),[21] 10(*Z*)-neosandalnol (**13**),[21] α-santalol (**14**),[15,22] (*E*)-α-santalal (**15**),[11] α-santaldiol (**16**),[23] α-santalenoic acid (**17**),[24] β-santalol (**18**),[15,25] (*E*)-β-santalal (**19**),[11] β-santaldiol (**20**),[24] and vanillic acid 4-*O*-neohesperidoside.[26]

Keywords: *Santalum album*; Santalaceae; Cancer chemoprevention; Campherenane-type sesquiterpene; Santalane-type sesquiterpene; Epstein–Barr virus; Mouse skin two-stage carcinogenesis.
* Corresponding author. Tel.: +81 86 251 7937; fax: +81 086 251 7926; e-mail: hito@cc.okayama-u.ac.jp

0040–4020/$ - see front matter © 2006 Elsevier Ltd. All rights reserved.
doi:10.1016/j.tet.2006.04.072

Table 1. ^{1}H NMR data for compounds **1**, **4**, **7**, **9**, and **12** in $CDCl_3$[a]

Position	1	4	7	9	11	12
1	—	—	—	—	—	1.89, m
2	4.06, ddd (9.6, 3 1.8)	3.64, dd (7.8, 3.6)	3.64, dd (7.2, 4.2)	3.29, d (1.8)	3.27, d (1.8)	—
3β	2.17, ddd (13.2, 9.6, 4.8)	1.65, ddd (13.2, 4.2, 3.6)	1.72, ddd (13.2, 4.2, 3.6)	—	—	—
3α	0.99, dd (13.2, 3)	1.75, dd (13.2, 7.8)	1.74, dd (13.2, 7.2)	—		
4	1.79, t (4.8)	1.85, br t (4.2)	1.87, br t (3.6)	1.76, br d (3)	1.84, br d (3.6)	1.82, br d (1.8)
5β	1.68, ddd (13.2, 9.6, 4.8)	1.61, dd (11.4, 3.6)	1.55, m	1.66, dddd (12, 9, 6, 3)	1.66, m	1.55, dddd (12.6, 9.6, 7.2, 1.8)
5α	1.26, ddd (13.2, 8.4, 3)	1.02, ddd (11.4, 9.6, 4.2)	1.05, m	1.66, dddd (12, 9, 6, 3)	1.66, m	1.25, dddd (12.6, 9.6, 6, 3.6)
6β	1.25, dddd (13.2, 9.6, 3, 1.8)	1.51, dt (12, 4.2)	1.54, m	1.04, ddd (11.4, 3, 1.8)	1.46, m	1.42, dddd (12, 9.6, 7.2, 3.6)
6α	1.88, ddd (13.2, 8.4, 4.8)	0.93, ddd (12, 9.6, 3.6)	0.95, m	1.59, ddd (11.4, 9, 6)	1.08, m	1.34, dddd (12, 9.6, 6, 2.4)
7	—	—	—	1.42, m; 1.14, dd (10.2, 1.2)	1.43, m; 1.18, dd (10.2, 1.8)	2.01, m; 1.06, br d (10.2)
8	1.36, dt (13.2, 4.8); 1.13, dt (13.2, 4.8)	1.93, dt (13.2, 4.8); 1.13, dt (13.2, 4.8)	1.30, dt (12.6, 4.8); 1.09, dt (12.6, 4.8)	1.35, ddd (13.8, 10.2, 6); 1.41, m	1.29, m	1.53, m; 1.31, m
9	2.15, ddd (12.6, 7.8, 4.8); 1.97, ddd (12.6, 7.8, 4.8)	2.09, ddd (13.2, 7.8, 4.8); 2.02, ddd (13.2, 7.8, 4.8)	2.22, ddd (12.6, 7.8, 4.8); 1.99, ddd (12.6, 7.8, 4.8)	2.15, m; 2.09, m	2.33, br dd (13.2, 7.2); 2.32, br dd (13.2, 7.2)	2.18, br dd (12.2, 6.6); 2.05, br dd (12.2, 6.6)
10	5.56, br t (7.8)	5.59, br t (7.8)	5.58, br t (7.8)	5.57, br t (7.2)	6.49, ddt (1.2, 2.4, 7.2)	5.59, br t (7.2)
11	—	—	—	—	—	—
12	4.32, br s	4.30, d (12.6); 4.24, d (12.6)	4.34, br s	4.34, d (12); 4.28, d (12)	1.75, m	4.34, d (12); 4.19, d (12)
13	4.21, br s	4.15, br s	4.22, br s	4.20, br s	9.39, s	4.18, s
14	0.85, s	0.90, s	0.91, s	1.08, s	1.10, s	1.21, s
15	0.89, s	0.84, s	1.04, br s	0.85, s	0.90, s	0.89, s

[a] Chemical shifts are shown in δ scale with J values (Hz) in parentheses.

2.1. Structures of new sesquiterpenoids

Compound **1** was isolated as a colorless oil, $[\alpha]_D^{20}$ −9.6 ($CHCl_3$). The molecular formula $C_{15}H_{26}O_3$ for **1** was determined from an ion peak at m/z 236.1767 $[M-H_2O]^+$ in HREIMS and NMR data described below. The ^{1}H NMR spectrum of **1** (Table 1) exhibited characteristic signals for two tertiary methyl groups at δ_H 0.89 (3H, s, H-15), 0.85 (3H, s, H-14), one oxygenated methine proton at δ_H 4.06 (1H, ddd, J=9.6, 3.0, 1.8 Hz, H-2), and a methine proton at δ_H 1.79 (1H, t, J=4.8 Hz, H-4), indicating the presence of a borneol moiety in **1**. The presence of the bicyclo[2.2.1]-heptane-2-ol skeleton was suggested by ^{13}C NMR resonance[27,28] (Table 2), which was further supported by cross peaks (H-3/H-2, -4 and H-5/H-4, -6) in the ^{1}H–^{1}H COSY, and long-range correlation of H-2/C-1, -3 and H-14/C-1, -2, -6 in the HMBC spectrum. The ^{1}H NMR spectrum revealed signals due to one olefinic proton at δ_H 5.56 (1H, br t, J=7.8 Hz, H-10), two hydroxymethylene groups at δ_H 4.32 (2H, br s, H-12), 4.21 (2H, br s, H-13), and four methylene protons at δ_H 2.15 (1H, ddd, J=12.6, 7.8, 4.8 Hz, H-9), 1.97 (1H, ddd, J=12.6, 7.8, 4.8 Hz, H-9), 1.36 (1H, dt, J=13.2, 4.8 Hz, H-8), 1.13 (1H, dt, J=13.2, 4.8 Hz, H-8). The ^{1}H–^{1}H COSY correlations of H-9/H-8, -10 and H-10/H-12, -13 confirmed the presence of a C_6 side chain as a comprising unit. The location of functional groups and the bulky aliphatic residue was further elucidated by key HMBC correlations of H-12/C-10, -11, -13, H-13/C-10, -11, -12, H-10/C-9, -11, -12, 13, and H-8/C-1, -4, -7, -9, -10, -15. The spectral data indicated the attached position of the methylene bridge on the bornane skeleton. The relative stereochemistry at C-7 and C-2 was determined by NOESY correlations of H-15/H-5β, H-2/H-14, -9, -8, and H-3β/H-9, -2. The *endo*-oriented secondary alcohol at C-2 was confirmed by comparison of the NMR chemical shift data of H-2 and C-2 (δ_H 4.06, δ_C 77.3) with those in the literature (for *exo*-OH; ca. δ_H 3.60, δ_C 80.0, for *endo*-OH; ca. δ_H 4.00, δ_C 77.0)[26–29] and significant W-type long-range coupling between H-2 and H-6β (J=1.8 Hz). The absolute configuration at C-2 in **1** was determined using the modified Mosher's method.[30,31] Compound **1** was treated with (*S*)-(+)- and (*R*)-(−)-α-methoxy-α-(trifluoromethyl)-phenylacetyl chloride in anhydrous pyridine at room temperature overnight to afford (*R*)- and (*S*)-MTPA ester derivatives (**1a** and **1b**, respectively). A negative value ($\Delta\delta_{S-R}$) was obtained for H-14 and positive difference values for H-3, -4 (Table 3),

Table 2. ^{13}C NMR data for compounds **1**, **4**, **7**, **9**, **11**, and **12** in $CDCl_3$[a]

Position	1	4	7	9	11	12
1	50.4	50.0	49.9	49.0	49.0	52.2
2	77.3	79.7	80.2	83.3	83.9	81.4
3	38.8	39.9	40.1	42.1	42.2	46.7
4	42.1	42.0	42.0	46.8	46.0	47.7
5	28.0	27.1	27.0	26.2	26.2	24.0
6	26.1	34.4	34.1	25.4	25.3	23.2
7	51.3	49.4	49.3	40.9	40.8	34.2
8	32.4	33.2	33.7	42.2	41.1	37.7
9	23.7	23.1	23.1	22.6	24.1	24.5
10	131.7	132.2	132.0	132.1	155.2	131.7
11	136.7	136.6	136.6	136.6	139.1	136.7
12	60.0	59.4	60.1	59.9	14.1	60.1
13	67.6	67.3	67.7	67.8	195.3	67.7
14	13.4	11.4	11.3	19.4	19.4	22.3
15	16.6	16.8	16.5	16.7	16.6	19.8

[a] Chemical shifts are shown in δ scale.

Table 3. Partial ^{1}H NMR data of the (*S*)- and (*R*)-Mosher esters of compounds **1**, **2**, **2c**, **9**, and **10** in $CDCl_3$[a]

Position	δ_H													
	1a	**1b**	$\Delta\delta_{S-R}$	**2a**	**2b**	$\Delta\delta_{S-R}$	**2d**	**2e**	$\Delta\delta_{S-R}$	**9a**	**9b**	$\Delta\delta_{S-R}$	**10a**	**10b**	$\Delta\delta_{S-R}$
2	5.13	5.10	*R*[b]	5.15	5.12	*R*[b]	5.16	5.11	*R*[b]	4.61	4.62	*R*[b]	4.62	4.63	*R*[b]
3β	2.29	2.28	+0.01	2.34	2.33	+0.01	2.38	2.38	±0	—	—	—	—	—	—
3α	1.14	1.03	+0.11	1.13	1.02	+0.11	1.15	1.05	+0.10	—	—	—	—	—	—
4	1.85	1.81	+0.04	1.88	1.84	+0.04	1.89	1.84	+0.05	1.66	1.68	−0.02	1.66	1.67	−0.01
5β	1.70	1.65	+0.05	1.69	1.66	+0.03	1.68	1.67	+0.01	1.62	1.62	±0	1.65	1.60	+0.05
5α	1.24	1.24	±0	1.23	1.17	+0.06	1.20	1.15	+0.05	1.30	1.33	−0.03	1.33	1.35	−0.02
6β	1.84	1.83	+0.01	1.82	1.82	±0	1.82	1.82	±0	1.57	1.53	+0.04	1.57	1.55	+0.02
6α	1.30	1.30	±0	1.31	1.31	±0	1.33	1.33	±0	1.07	1.00	+0.07	1.06	1.00	+0.06
7	—	—	—	—	—	—	—	—	—	1.48	1.48	±0	1.46	1.47	−0.01
	—	—	—	—	—	—	—	—	—	1.16	1.16	±0	1.15	1.16	−0.01
14	0.80	0.87	−0.07	0.80	0.87	−0.07	0.80	0.88	−0.08	1.06	0.98	+0.08	1.06	0.98	+0.08
15	0.87	0.87	±0	0.88	0.88	±0	0.89	0.89	±0	0.68	0.76	−0.08	0.65	0.74	−0.09

[a] Data were assigned on the basis of the correlation with 2D NMR spectroscopy.
[b] Absolute configuration.

establishing that the absolute configuration of the chiral center at C-2 is *R*. Therefore, the structure of compound **1** was fully assigned to (2*R*,7*R*)-2,12,13-trihydroxy-10-campherene.

The HREIMS of compound **4**, $[\alpha]_D^{20}$ +15.7 ($CHCl_3$), showed a pseudomolecular ion peak at *m/z* 236.1775 $[M-H_2O]^+$, indicating that the molecular formula ($C_{15}H_{26}O_3$) is the same as that of **1**. The ^{1}H and ^{13}C NMR spectral data of **4** (Tables 1 and 2) were also analogous to those of **1** except for H-2 and H-3 signals. Remarkable upfield shift of H-2 (Δδ, 0.42 ppm) and downfield shift of C-2 (Δ 2.40 ppm) were observed in **4** compared with **1**. These spectral characteristics suggested the presence of an *exo*-OH group at C-2.[27–29] In addition, relative stereochemistry was inferred by NOE cross peaks of H-15/H-6β, -5β, and H-2α/H-6α, -3α. We attempted the determination of the absolute configuration at C-2 by modified Mosher's method.[30,31] However, MTPA esters of **4** were not obtained probably because of steric hindrance between the hydroxyl group at C-2 and the side chain. The absolute structure **4** was proposed by comparing its specific optical rotation with that of compound **1**, with reference to synthetic campherenol (**3**) ($[\alpha]_D$ −5.3) and isocampherenol (**6**) ($[\alpha]_D$ +25.0),[32] unless the presence of hydroxyl groups in the side chain influenced the sign of specific rotation. Thus, compound **4** was assigned to (2*S*,7*R*)-2,12,13-trihydroxy-10-campherene, which is the C-2 epimer of **1**.

Although compounds **2**, **5**, and **10** were recently reported as constituents of commercial sandalwood,[21] their absolute structures remained unassigned. We have established the absolute stereostructures of **2** and **10** as shown in Figure 1 by a combination of NOESY experiment and modified

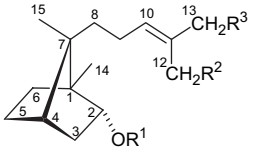

Compd.	R^1	R^2	R^3
1	H	OH	OH
1a	(*S*)-MTPA	*O*-(*S*)-MTPA	*O*-(*S*)-MTPA
1b	(*R*)-MTPA	*O*-(*R*)-MTPA	*O*-(*R*)-MTPA
2	H	OH	H
2a	(*S*)-MTPA	*O*-(*S*)-MTPA	H
2b	(*R*)-MTPA	*O*-(*R*)-MTPA	H
2c	H	*O*-CPh_3	H
2d	(*S*)-MTPA	*O*-CPh_3	H
2e	(*R*)-MTPA	*O*-CPh_3	H
3	H	H	H

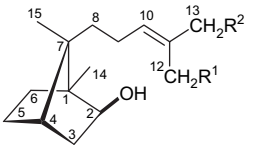

Compd.	R^1	R^2
4	OH	OH
5	OH	H
6	H	H

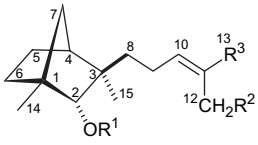

Compd.	R^1	R^2	R^3
9	H	OH	CH_2OH
9a	(*S*)-MTPA	*O*-(*S*)-MTPA	CH_2O-(*S*)-MTPA
9b	(*R*)-MTPA	*O*-(*R*)-MTPA	CH_2O-(*R*)-MTPA
10	H	OH	CH_3
10a	(*S*)-MTPA	*O*-(*S*)-MTPA	CH_3
10b	(*R*)-MTPA	*O*-(*R*)-MTPA	CH_3
11	H	H	CHO

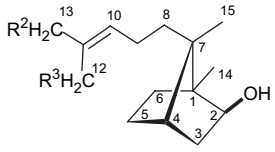

Compd.	R^1	R^2
7	OH	OH
8	H	H

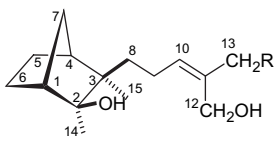

12: R = OH
13: R = H

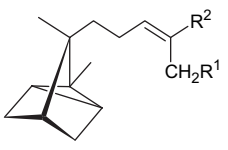

Compd.	R^1	R^2
14	OH	CH_3
15	H	CHO
16	OH	CH_2OH
17	H	COOH

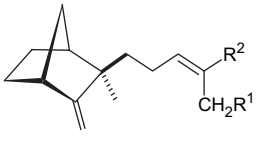

Compd.	R^1	R^2
18	OH	CH_3
19	H	CHO
20	OH	CH_2OH

Figure 1.

Mosher's method (Table 3). The absolute structure of **5**, whose relative structure was determined by NOESY, was deduced by comparing its specific rotation ($[\alpha]_D^{20}$ −17.6) with that of compound **2** ($[\alpha]_D^{20}$ +17.0) in an argument similar to that between **1** and **4**. Hence, compounds **2**, **5**, and **10** were assigned to (2*R*,7*R*)- and (2*S*,7*R*)-2,12-dihydroxy-10(*Z*)-campherene, and (2*R*,3*R*)-10(*Z*)-sandalnol, respectively.

The molecular formula $C_{15}H_{26}O_3$ of **7** was determined by its HREIMS. Both the ^{1}H and ^{13}C NMR data of compound **7** (Tables 1 and 2) were very similar to those of **4**, however, large chemical shift differences for CH_3-15 and H-8, and the appearance of CH_2-12 as a broad singlet were distinguishing features from **4**. In addition, clear correlations were observed between H-8 and H-6β, -5β in the NOESY experiment of **7**, whereas no correlation was observed between H-15 and H-6β, -5β. These 1D- and 2D-NMR data for **7** suggested that the orientation of the side chain at C-7 was opposite to that of **4**. Thus, compound **7** was characterized to be (2*S**,7*S**)-2,12,13-trihydroxy-10-campherene.

Compound **9** was obtained as a colorless oil, $[\alpha]_D^{20}$ −4.8 ($CHCl_3$). The molecular formula $C_{15}H_{26}O_3$, which was the same as that of **1**, **4**, and **7**, was deduced from NMR data and a pseudomolecular ion peak $[M-H_2O]^+$ at *m*/*z* 236.1773 in HREIMS. In the ^{1}H NMR spectrum of **9** (Table 1), the doublet signal at δ_H 3.29 (1H, d, *J*=1.8 Hz, H-2) attributable to an oxygenated methine proton, clearly differed from the corresponding signals of **1**, **4**, and **7**. One (δ_H 1.08, H-14) of the two tertiary methyl groups also showed downfield shift (ca. 0.2 ppm) relative to those of the above three compounds, suggesting that compound **9** is not a campherene analogue. The presence of an α-fenchol framework as a partial structure was indicated by the close similarity of ^{13}C NMR resonances to the data reported for α-fenchol,[33] as well as by HMBC correlations of H-2/C-1, -3, -14, H-8/C-2, -4, -10, -15, H-14/C-2, -6, -7, and H-15/C-2, -4, -8. Also, the existence of an oxygenated prenyl group as the other constituent unit in **9** was substantiated by spectral resemblance to the corresponding signals in ^{1}H and ^{13}C NMR spectra of **1**, **4**, and **7**. The NOE correlations of H-2/H-7, -8, -14, and H-15/H-5α in **9** indicated the cis relationship of 2-OH and 3-CH_3 groups. The 2*R* configuration was confirmed by the modified Mosher's method (Table 3). Therefore, the structure of **9** was determined to be (2*R*,3*R*)-13-hydroxysandalnol.

The ^{1}H and ^{13}C NMR data (Tables 1 and 2) of compound **11**, $[\alpha]_D^{20}$ −5.1 ($CHCl_3$), were similar to those of **10**, and the only difference was observed in the presence of an aldehyde signal [δ_H 9.39 (1H, s), δ_C 195.3] instead of the methyl signal in **10**. The 2D-NMR analysis and HREIMS data (*m*/*z* 236.1773 $[M]^+$, $C_{15}H_{24}O_2$) showed the structure **11** for this compound. The *E* configuration of the double bond in **11** was assigned by significant NOE of the aldehyde proton (H-13) with H-10 as well as the correlation between H-12 and H-9 in the NOESY spectrum. The chemical shift of H-13 (δ_H 9.39) was also consistent with the trans-oriented α,β-unsaturated aldehyde proton signal generally accepted (δ_H 9.33 for trans, δ_H 10.2 for cis-oriented CHO).[9] Taking the biogenetic pathway into consideration, the stereostructure of **11** was tentatively assigned to (2*R**,3*R**)-10(*E*)-sandalnol-13-al.

Compound **12**, $[\alpha]_D^{20}$ −63.6 ($CHCl_3$), exhibited an ion peak $[M-H_2O]^+$ at *m*/*z* 236.1768 in HREIMS, corresponding to the molecular formula $C_{15}H_{26}O_3$. The ^{1}H NMR spectrum of **12** (Table 1) revealed signals assignable to two tertiary methyl protons at δ_H 0.89 and 1.21 (3H each, s, H-15, -14, respectively), two methine protons at δ_H 1.89 (1H, m, H-1), 1.82 (1H, br d, *J*=1.8 Hz, H-4), a methylene-bridge proton at δ_H 2.01 (1H, m, H-7), 1.06 (1H, br d, *J*=10.2 Hz, H-7), a vinyl proton at δ_H 5.59 (1H, br t, *J*=7.2 Hz, H-10), and two hydroxymethylene protons at δ_H 4.19, 4.34 (1H each, d, *J*=12.0 Hz, H-12), δ_H 4.18 (2H, s, H-13) arising from methylene bicyclo[2.2.1]heptane moiety and C_6 side chain unit. These data resemble to those for β-santaldiol (**20**)[23] except for the presence of 2-OH and 14-CH_3 groups instead of the exomethylene group in **20**. The relative configuration of **12** was determined by key NOESY correlations (H-15/H-14, -5α, H-14/H-15, -6α, and H-8/H-7). Thus, compound **12** was characterized to be (2*S**,3*R**)-13-hydroxy-neosandalnol.

Compound **13**, $[\alpha]_D^{20}$ −26.7 ($CHCl_3$) was previously reported to have a planar structure.[21] The transformation from compound **13** into the dehydrated derivative was observed by NMR measurement of $CDCl_3$ overnight, although the cause for this phenomenon remains uncertain. The dehydrate ($[\alpha]_D^{20}$ −90.3) was identified to be β-santalol (**18**) by NMR and MS analyses, and also by comparison with an authentic specimen. On the basis of this finding, the stereostructure of **13** was assigned to (2*S*,3*R*)-10(*Z*)-neosandalnol.

Campherenane and santalane derivatives have been found in certain species of Illiciaceae,[27] Lauraceae,[28] Rutaceae,[34] Hepaticae,[35] and Santalaceae,[8–11,23,36,37] even though they are very rare classes of sesquiterpenes. These metabolites with diverse structures were presumed to be derived from bisabolol via santalenes including Wagner–Meerwein rearrangement and oxidation steps.

2.2. Structures of new aromatic glycosides

The HRESIMS of compound **21** gave a pseudomolecular ion $[M+NH_4]^+$ at *m*/*z* 490.2280, consistent with the molecular formula of $C_{22}H_{32}O_{11}$. The ^{1}H NMR spectrum of **21** showed signals attributable to 1,3,4-trisubstituted-type aromatic protons at δ_H 7.06 (1H, d, *J*=8.4 Hz, H-5), 6.83 (1H, d, *J*=1.8 Hz, d, H-2), 6.72 (1H, dd, *J*=8.4, 1.8 Hz, H-6), terminal monosubstituted double-bond protons at δ_H 6.00 (1H, m, H-8), 5.01, 5.07 (1H each, m, H-9), a methylene proton at δ_H 3.36 (2H, d, *J*=6.6 Hz, H-7), and a methoxyl group at δ_H 3.85 (3H, s). These signals suggest the presence of a C_6–C_3 moiety, which was substantiated by the HSQC experiment. In addition to aglycone signals, two characteristic anomeric signals at δ_H 5.39 and 5.06, and 11 oxygen-bearing protons at δ_H 4.16–3.38 were observed, along with a doublet methyl signal at δ_H 1.25, indicating the presence of glucose and rhamnose moieties.[26,38] These NMR data in combination with the observed ^{1}H–^{1}H COSY correlations (Fig. 2) suggested that compound **21** is a simple phenolic rhamnoglucoside. The glycosidic linkage of the sugar moiety was determined to be β for glucose and α for rhamnose from the coupling constants of 7.8 and 1.8 Hz for anomeric protons, respectively. The presence of a β-glucosyl and an

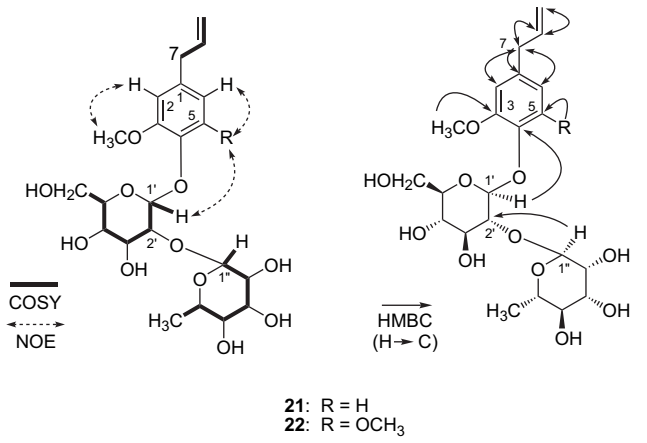

Figure 2. Selected COSY, HMBC, and NOESY correlations of compounds **21** and **22**.

α-rhamnosyl moieties was further evidenced by the ^{13}C NMR spectrum (Table 4).[39–41] These assignments of sugar linkages and the position of a methoxyl group were confirmed unambiguously from HMBC (H-1′/C-4, H-1″/C-2′, and OCH_3/C-3) and NOESY (H-1′/H-5 and OCH_3/H-2) experiments (Fig. 2). Acid hydrolysis of compound **21** gave eugenol, which was confirmed by direct comparison of HPLC and reported NMR data with those of an authentic sample.[42,43] Unfortunately, the limited amount of **21** obtained did not allow elucidation of the absolute configuration of its sugar moiety. Thus, the structure of compound **21** was determined to be a new phenolic glycoside, eugenol 4-*O*-rhamnosyl(1→2)glucoside.

Table 4. NMR spectroscopic data for compounds **21** and **22** in CD_3OD[a]

Position	δ_H		δ_C	
	21	**22**	**21**	**22**
Aglycone moiety				
1			139.1	136.8
2	6.83, d (1.8)	6.54, s	113.8	106.4
3			151.3	153.2
4			145.8	132.9
5	7.06, d (8.4)		118.2	153.2
6	6.72, dd (8.4, 1.8)	6.54, s	121.5	106.4
7	3.36, d (6.6)	3.37, m	40.8	40.1
8	6.00, m	6.00, m	136.7	137.6
9	5.07, m; 5.01, m	5.15, m; 5.08, m	115.7	114.9
OCH_3	3.85, 3H, s	3.86, 6H, s	56.3	55.8
Glucose moeity				
1′	5.06, d (7.8)	5.12, d (7.2)	100.7	101.4
2′	3.75, dd (9.0, 7.2)	3.72, dd (9.0, 7.2)	78.5	78.7
3′	3.63, t (9.0)	3.56, t (9.0)	79.5	77.9
4′	3.41, m	3.49, m	71.5	70.2
5′	3.38, m	3.20, m	78.0	76.7
6′	3.87, dd (12.0, 2.4)	3.77, dd (11.4, 2.4)	62.5	61.4
6′	3.68, m	3.67, dd (11.4, 4.8)		
Rhamnose moiety				
1″	5.39, d (1.8)	5.25, d (1.8)	102.0	101.3
2″	3.98, dd (3.6, 1.8)	4.02, dd (3.6, 1.8)	72.4	71.3
3″	3.70, m	3.81, dd (9.6, 3.6)	72.2	71.5
4″	3.40, m	3.42, t (9.6)	74.0	72.7
5″	4.16, dd (9.6, 6.6)	4.20, dd (9.6, 6.6)	70.0	68.6
6″	1.25, d (6.6)	1.14, d (6.6)	18.1	16.4

[a] Chemical shifts are shown in δ scale with J values (Hz) in parentheses.

Compound **22**, $[\alpha]_D^{20}$ −111.6 (*c* 0.1, MeOH), was obtained as a yellowish syrup. The molecular formula was determined to be $C_{23}H_{34}O_{12}$ by HRESIMS (*m*/*z* 525.1937, $[M+Na]^+$), which was 30 mass units larger than **21**. The ^1H and ^{13}C NMR spectra of **22** (Table 4) were very similar to those of **21**, except for the presence of an extra methoxyl signal [δ_H 3.86 (6H, s), δ_C 55.8, C-5] and a magnetically equivalent 2H-singlet (δ_H 6.54) instead of the ABX aromatic signals in **21**. The structure of **22**, including relative stereochemistry and identity of the aglycone moiety, was determined in a manner similar to that of **21**. The hydrolyzate of **22** obtained upon treatment with acid was identified as methoxyeugenol by comparison with the reported NMR data and direct HPLC comparison with a commercial authentic sample.[44] As a result, the new compound **22** was assigned to be methoxyeugenol 4-*O*-rhamnosyl(1→2)glucoside. Isolation of aromatic neohesperidosides from the genus *Santalum* might thus be of chemotaxonomical significance (Fig. 2).

2.3. Antitumor activity of the isolates from *S. album*

Owing to the immensely rare occurrence of this type of compound in the plant kingdom, the only α-santalol (**14**) has been assessed for biological activities in several bioassays.[13–16] The remarkable antitumor promoting effect of α-santalol (**14**)[17] prompted us to examine the antitumor effects of the purified constituents from *S. album* of Indian origin in vitro and in vivo. The inhibitory effects of the isolates on EBV-EA activation induced by 12-*O*-tetradecanoylphorbol-13-acetate (TPA), which is a short-term in vitro screening method frequently used to survey possible antitumor promoters in nature, were assessed. As shown in Table 5, compounds **1**, **4**, and **20** among the tested compounds showed a remarkable inhibitory effect on EBV-EA activation of 63.9, 62.3, and 61.8% inhibition, respectively, at a concentration of 500 mol ratio/TPA, preserving high cell viability. These potencies were comparable to that of the positive control, (−)-epigallocatechin gallate (EGCG), which is a well-known antitumor promoting polyphenol from green tea.[45,46] On the basis of the in vitro results, the potent inhibitors **1**, **18**, and **20**, which were well supplied for the in vivo test, were further assessed for the suppression of two-stage mouse skin carcinogenesis induced by 7,12-dimethylbenz[*a*]anthracene (DMBA) as an initiator and TPA as a promoter. The activity was evaluated in terms of both the rate (%) of papilloma-bearing mice (Fig. 3A) and the average number papillomas per mouse (Fig. 3B) compared with that of the control. The control showed that 100% of the mice bore papillomas after 10 weeks of promotion, whereas treatment with compounds **1**, **18**, and **20** along with the initiator and promoter reduced the percentages of tumor-bearing mice to 33.4–46.7% even at 15 weeks. Among them, compound **1** had the most potent activity, reducing the incidence to 86.6% over 20 weeks. Furthermore, in the treated group, the average number of papillomas per mouse was also reduced to about 50% relative to the control group over 20 weeks. The results of this investigation indicated that compounds **1**, **18**, and **20** might be other potential antitumor promoters of sandalwood and valuable for further study for a possible antitumor promoting mechanism.

Table 5. Relative ratio[a] of EBV-EA activation with respect to positive control (100%) in the presence of isolates from *Santalum album*

Compound	EBV-EA–positive cells % to control (% viability): compounds concentration (mol ratio/32 pmol TPA)			
	1000	500	100	10
Sesquiterpenoids				
1	0.0±0.2 (60)[b]	36.1±1.9	71.3±1.9	88.4±0.5
2	0.0±0.3 (60)	41.5±2.0	74.9±2.2	92.6±0.7
4	0.0±0.2 (60)	37.7±1.9	72.0±2.0	89.9±0.6
14	0.0±0.4 (60)	47.7±2.3	76.8±2.5	93.0±0.9
16	0.0±0.3 (60)	40.8±2.1	73.7±2.2	91.3±0.6
18	0.0±0.3 (60)	44.3±2.1	74.2±2.1	92.1±0.9
20	0.0±0.2 (60)	38.2±2.0	72.7±2.1	90.5±0.6
(+)-α-Nuciferol[c]	0.0±0.4 (70)	49.2±2.3	78.5±2.2	96.8±0.4
Neolignans[c]				
(7*S*,8*S*)-$\Delta^{7'}$-4,5,9,9′-Tetrahydroxy-3,5-dimethoxy-7-*O*-5′,8′-*O*-4′-neolignan	0.0±0.4 (70)	48.0±2.2	77.4±2.1	94.5±0.7
Diethylene glycol monobenzoate	12.7±0.6 (60)	68.5±2.5	87.1±2.6	100±0.3
(−)-Secoisolariciresinol	2.1±0.4 (60)	52.3±2.1	79.6±2.0	96.4±0.4
(7′*S*,8*R*,8′*R*)-Lyoniresinol	8.4±0.5 (60)	55.7±2.4	85.3±2.6	100±0.2
(7*S*,8*S*)-3-Methoxy-3′,7-epoxy-8,4′-oxyneoligna-4,9,9′-triol	0.0±0.4 (70)	49.2±2.3	78.6±2.0	94.9±0.7
Dihydrodehydrodiconiferyl alcohol	3.5±0.4 (70)	53.7±2.2	82.8±2.1	100±0.4
(−)-EGCG[d]	6.4±0.8 (70)	34.9±1.3	68.1±2.1	87.7±0.9

[a] Values represent percentages relative to the positive control value (100%).
[b] Values in parentheses are the viability percentages of Raji cells; unless otherwise stated, the viability percentages of Raji cells were more than 80%.
[c] See Refs. 19 and 20.
[d] Positive control substance.

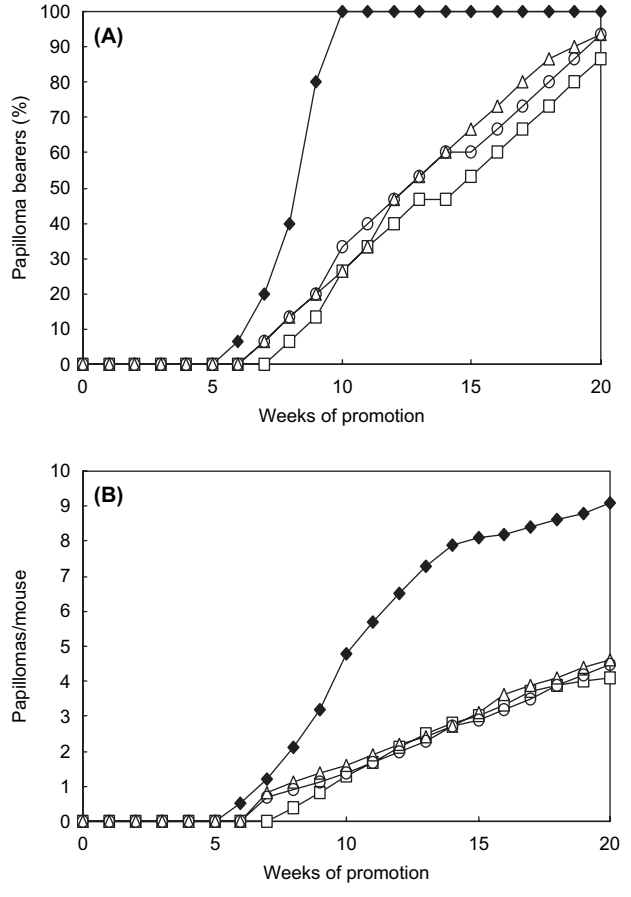

Figure 3. Inhibition of TPA-induced tumor promotion by multiple applications of **1**, **18**, and **20**. All mice were initiated with DMBA (390 nmol) and promoted with 1.7 nmol of TPA given twice weekly starting one week after initiation. (A) Percentage of mice bearing papillomas. (B) Average numbers of papillomas per mouse. ◆, control (TPA alone); □, TPA+**1**; ○, TPA+**18**; △, TPA+**20**.

3. Experimental

3.1. General

Optical rotations were measured with a JASCO DIP-4 digital polarimeter. The ^{1}H and ^{13}C NMR spectra were measured on a Varian Unity Inova AS600NB instrument operating at 600 and 150 MHz, respectively. The chemical shifts are given in δ (ppm) values relative to those of the solvents $CDCl_3$ (δ_H 7.26; δ_C 77.0) and CD_3OD (δ_H 3.35; δ_C 49.0) on a tetramethylsilane (TMS) scale. The standard pulse sequences programmed into the instruments were used for each 2D measurement. The J_{CH} value was set at 8 Hz in the HMBC spectra. HRESIMS and ESIMS were obtained on a Micro Mass Auto Spec OA-TOF spectrometer (solvent: 50% MeOH containing 0.1% $AcONH_4$; flow rate: 0.02 ml/min). Normal-phase HPLC was conducted on a YMC-Pack SIL A-003 column (4.6 mm i.d.×250 mm; YMC Co. Ltd) and developed at room temperature with a solvent of *n*-hexane–EtOH (15:1) (flow rate: 1.5 ml/min; detection: UV 205 or 220 nm) or *n*-hexane–EtOH (3:1) (flow rate: 1.5 ml/min; detection: UV 280 nm). Reversed-phase HPLC was carried out on a YMC-Pack ODS A-302 column (4.6 mm i.d.×150 mm; YMC Co., Ltd) and developed at 40 °C with 10 mM H_3PO_4/10 mM KH_2PO_4/CH_3CN (7:3) (flow rate: 1.0 ml/min; detection: UV 205 or 220 nm) or 10 mM H_3PO_4/10 mM KH_2PO_4/CH_3CN (9:1) (flow rate: 1.0 ml/min; detection: UV 280 nm). Column chromatography was carried out on silica gel 60 (Merck, 70–230 mesh), Toyopearl HW-40 (coarse grade; Tosoh Co.), YMC GEL ODS AQ 120-50S (YMC Co., Ltd), MCI GEL CHP-20P (Mitsubishi Kasei Co.), and Sephadex LH-20 (Pharmacia Fine Chemicals Co., Ltd). Preparative TLC was performed on Kieselgel 60 F_{254} plates (0.2 mm layer thickness, Merck).

3.2. Plant material

Chips of *S. album* L. wood collected in Mysore district of India were used. The wood was officially imported from

India under a special treaty between the Indian and Japanese governments to sculpt a Buddhist image in a Japanese temple (Kannonshoji Temple) with a long and distinguished history.

3.3. Extraction and isolation

The heartwood of *S. album* (1.53 kg) was extracted with MeOH at room temperature. The combined crude MeOH extract (73.1 g) was suspended in 20% MeOH (2 l), and then partitioned in turn with *n*-hexane (3×2 l) and EtOAc (3×2 l) to afford dried *n*-hexane- (16.4 g), EtOAc- (27.1 g), and H_2O-soluble (17.5 g) residues. On performing the chromatographic separation, fractions were monitored with normal and reversed-phase HPLC. The *n*-hexane extract (10.0 g) was subjected to silica gel column chromatography (6.0 cm i.d.×42 cm, 70–230 mesh) using *n*-hexane containing increasing amounts of EtOAc in a stepwise gradient to give 12 pools. The eluates of *n*-hexane–EtOAc (9:1) and *n*-hexane–EtOAc (85:15) were subjected to preparative reversed-phase HPLC (YMC-Pack ODS-AM, 20.0 mm i.d.×250 mm) with 70% aqueous CH_3CN, to give α-santalol (**14**) (105.3 mg), (*E*)-α-santalal (**15**) (20.0 mg), (*E*)-β-santalal (**19**) (23.3 mg), and β-santalol (**18**) (111.0 mg). Similarly, the *n*-hexane–EtOAc (1:1) and *n*-hexane–EtOAc (3:2) eluates were purified by preparative reversed-phase HPLC with 40% aqueous CH_3CN to afford pure α-santaldiol (**16**) (98.7 mg), α-santalenoic acid (**17**) (18.0 mg), and β-santaldiol (**20**) (91.4 mg), as well as a crude fraction containing compounds **2**, **5**, **10**, **11**, and **13**. This crude fraction was finally purified by preparative normal-phase HPLC (4.6 mm i.d.×250 mm) developed with *n*-hexane–EtOH (15:1), and yielded pure compounds **2** (23.5 mg, t_R 10.1 min), **5** (7.5 mg, t_R 9.3 min), **10** (3.5 mg, t_R 12.9 min), **11** (2.6 mg, t_R 9.5 min), and **13** (26.6 mg, t_R 4.68 min). A part (7.0 g) of the EtOAc extract was chromatographed on a Toyopearl HW-40 column (coarse grade; 2.2 cm i.d.×65 cm) with H_2O containing increasing amounts of MeOH in a stepwise gradient mode. The 40% MeOH eluate was subjected separately to column chromatography over a YMC GEL ODS AQ 120-50S column (1.1 cm i.d.×41 cm) with aqueous MeOH, and finally purified by preparative normal-phase HPLC (4.6 mm i.d.×250 mm) developed with *n*-hexane–EtOH (15:1), yielding pure compounds **1** (29.0 mg, t_R 27.7 min), **4** (25.3 mg, t_R 22.3 min), **10** (1.8 mg, t_R 33.5 min), **9** (7.4 mg, t_R 18.3 min), and **12** (9.4 mg, t_R 15.6 min). A part (3.0 g) of the H_2O soluble residue was chromatographed over a Diaion HP-20 column (3.2 cm i.d.×35 cm) with H_2O containing increasing amounts of MeOH in a stepwise gradient mode. The 60% MeOH eluate was subjected separately to column chromatography over Sephadex LH-20 (1.1 cm i.d.×38 cm) with MeOH and YMC GEL ODS AQ 120-50S column (1.1 cm i.d.×41 cm) with aqueous MeOH, and finally purified by preparative normal-phase HPLC (4.6 mm i.d.×250 mm) developed with *n*-hexane–EtOH (3:1) to yield pure compounds **21** (2.3 mg, t_R 33.7 min) and **22** (1.3 mg, t_R 27.1 min), and vanillic acid 4-*O*-neohesperidoside (1.7 mg, t_R 5.3 min).

3.3.1. (2*R*,7*R*)-2,12,13-Trihydroxy-10-campherene (1). Colorless oil; $[\alpha]_D^{20}$ −9.6 (*c* 1.0, $CHCl_3$); ^1H and ^{13}C NMR, see Tables 1 and 2; EIMS *m/z* 236 $[M-H_2O]^+$ (15), 218 (42), 200 (31), 185 (16), 161 (20), 145 (6), 121 (78), 95 (100); HREIMS *m/z* 236.1767 $[M-H_2O]^+$ (calcd for $C_{15}H_{26}O_3-H_2O$, 236.1776).

3.3.2. (2*R*,7*R*)-2,12-Dihydroxy-10(*Z*)-campherene (2). Colorless oil; $[\alpha]_D^{20}$ −17.6 (*c* 0.1, $CHCl_3$); ^1H and ^{13}C NMR, see Tables 1 and 2; EIMS *m/z* 238 $[M]^+$ (13), 220 (35), 202 (41), 187 (18), 159 (32), 145 (37), 121 (51), 91 (82), 58 (100); HREIMS *m/z* 238.1941 $[M]^+$ (calcd for $C_{15}H_{26}O_2$, 238.1933).

3.3.3. (2*S*,7*R*)-2,12,13-Trihydroxy-10-campherene (4). Colorless oil; $[\alpha]_D^{20}$ +15.7 (*c* 0.5, $CHCl_3$); ^1H and ^{13}C NMR, see Tables 1 and 2; EIMS *m/z* 236 $[M-H_2O]^+$ (8), 218 (35), 200 (43), 185 (21), 161 (18), 145 (33), 121 (80), 91 (100); HREIMS *m/z* 236.1775 $[M-H_2O]^+$ (calcd for $C_{15}H_{26}O_3-H_2O$, 236.1776).

3.3.4. (2*S*,7*R*)-2,12-Dihydroxy-10(*Z*)-campherene (5). Colorless oil; $[\alpha]_D^{20}$ +17.9 (*c* 0.1, $CHCl_3$); ^1H and ^{13}C NMR, see Tables 1 and 2; EIMS *m/z* 238 $[M]^+$ (10), 220 (17), 202 (21), 187 (13), 159 (18), 145 (17), 121 (35), 91 (53), 58 (100); HREIMS *m/z* 238.1923 $[M]^+$ (calcd for $C_{15}H_{26}O_2$, 238.1933).

3.3.5. (2*S*,7*S*)-2,12,13-Trihydroxy-10-campherene (7). Colorless oil; $[\alpha]_D^{20}$ −4.6 (*c* 0.5, $CHCl_3$); ^1H and ^{13}C NMR, see Tables 1 and 2; EIMS *m/z* 236 $[M-H_2O]^+$ (13), 218 (61), 200 (53), 189 (38), 161 (32), 145 (42), 121 (87), 95 (100); HREIMS *m/z* 236.1771 $[M-H_2O]^+$ (calcd for $C_{15}H_{26}O_3-H_2O$, 236.1776).

3.3.6. (2*R*,3*R*)-13-Hydroxysandalnol (9). Colorless oil; $[\alpha]_D^{20}$ −4.8 (*c* 1.0, $CHCl_3$); ^1H and ^{13}C NMR, see Tables 1 and 2; EIMS *m/z* 236 $[M-H_2O]^+$ (8), 218 (21), 200 (37), 185 (20), 157 (43), 121 (72), 91 (78), 58 (100); HREIMS *m/z* 236.1773 $[M-H_2O]^+$ (calcd for $C_{15}H_{26}O_3-H_2O$, 236.1776).

3.3.7. (2*R*,3*R*)-10(*Z*)-Sandalnol (10). Colorless oil; $[\alpha]_D^{20}$ −7.3 (*c* 1.0, $CHCl_3$); ^1H and ^{13}C NMR, see Tables 1 and 2; EIMS *m/z* 238 $[M]^+$ (22), 220 (16), 202 (11), 187 (7), 159 (27), 145 (26), 138 (38), 121 (31), 110 (35), 91 (30), 81 (100); HREIMS *m/z* 238.1927 $[M]^+$ (calcd for $C_{15}H_{26}O_2$, 238.1933).

3.3.8. (2*R,3*R**)-10(*E*)-13-Sandalnol-13-al (11).** Colorless oil; $[\alpha]_D^{20}$ −5.1 (*c* 1.0, $CHCl_3$); ^1H and ^{13}C NMR, see Tables 1 and 2; EIMS *m/z* 236 $[M]^+$ (15), 218 (21), 200 (31), 155 (37), 121 (100), 91 (81); HREIMS *m/z* 236.1773 $[M]^+$ (calcd for $C_{15}H_{24}O_2$, 236.1776).

3.3.9. (2*S,3*R**)-13-Hydroxyneosandalnol (12).** Colorless oil; $[\alpha]_D^{20}$ −63.6 (*c* 1.0, $CHCl_3$); ^1H and ^{13}C NMR, see Tables 1 and 2; EIMS *m/z* 236 $[M-H_2O]^+$ (15), 218 (21), 200 (31), 185 (18), 157 (37), 91 (100); HREIMS *m/z* 236.1768 $[M-H_2O]^+$ (calcd for $C_{15}H_{26}O_3-H_2O$, 236.1776).

3.3.10. (2*S*,3*R*)-10(*Z*)-Neosandalnol (13). Colorless oil; $[\alpha]_D^{20}$ −26.7 (*c* 1.0, $CHCl_3$); ^1H and ^{13}C NMR, see Tables 1 and 2; 238 $[M]^+$ (17), 220 (16), 202 (62), 187 (22), 159 (35), 145 (30), 121 (68), 91 (82), 58 (100); HREIMS *m/z* 238.1926 $[M]^+$ (calcd for $C_{15}H_{26}O_2$, 238.1933).

3.3.11. Eugenol 4-*O*-rhamnosyl(1→2)glucoside (21). Colorless syrup, $[\alpha]_D^{20}$ −118.0 (*c* 0.1, MeOH); ^1H and ^{13}C NMR data, see Table 4; ESIMS *m/z* 490 $[M+NH_4]^+$; HRESIMS *m/z* 490.2280 $[M+NH_4]^+$ (calcd for $C_{22}H_{32}O_{11}+NH_4$, 490.2288).

3.3.12. Methoxyeugenol 4-*O*-rhamnosyl(1→2)glucoside (22). Yellowish syrup, $[\alpha]_D^{20}$ −111.6 (*c* 0.1, MeOH); ^1H and ^{13}C NMR data, see Table 4; ESIMS *m/z* 525 $[M+Na]^+$; HRESIMS *m/z* 525.1937 $[M+Na]^+$ (calcd for $C_{23}H_{34}O_{12}+Na$, 520.1948).

3.4. Tritylation of 2

Compound **2** (5.0 mg) and triphenyl methyl chloride (10.0 mg) were dissolved in 200 μl of dried pyridine, and the mixture was allowed to stand for 48 h at room temperature. Preparative TLC of the crude tritylation product obtained after the usual workup afforded 4.0 mg of tritylated derivative (**2c**) as a colorless oil.

3.5. Preparation of (*S*)- and (*R*)-MTPA ester derivatives of 1, 2, 2c, 9, and 10

Two portions each (each 1–1.5 mg) of compounds **1**, **2**, **2c**, **9**, and **10** were treated with (*S*)-(+)- and (*R*)-(−)-α-methoxy-α-(trifluoromethyl)-phenylacetyl chloride (10 μl) in anhydrous pyridine (200 μl) at room temperature overnight. The reaction mixtures were purified by preparative TLC with *n*-hexane–acetone (4:1) as developing solvent to afford (*R*)- and (*S*)-MTPA ester derivatives (**1a**, **1b**, **2a**, **2b**, **2d**, **2e**, **9a**, **9b**, **10a**, and **10b**) of **1**, **2**, **2c**, **9**, and **10**. Calculation of the differences of chemical shifts allowed the assignment of absolute stereochemistry of the respective original compound (Table 3).

3.6. Acid hydrolysis of 21 and 22

A solution of **21** (1.0 mg) [or **22** (0.7 mg)] in 1 M HCl (1 ml) was heated for 1 h in a boiling water bath. After cooling, the reaction mixture was separated using Mega Bond Elut C_{18} (Varian, USA) cartridge column to yield aglycone, eugenol (0.5 mg) [or methoxyeugenol (0.3 mg)] from the MeOH eluate. These aglycones were identified by HPLC comparison with authentic samples and spectral data with those reported in the literature.[42–44]

3.7. Assay for inhibition of EBV-EA activation

The inhibition of EBV-EA activation was assayed using Raji cells (virus nonproducer) as described previously.[47,48] The EBV genome carrying lympoblastoid cells was derived from Burkitt's lymphoma, which was cultured in 10% fetal bovine serum (FBS) in RPMI-1640 medium (Nissui, Japan). Spontaneous EBV-EA activation in our Raji cell subline was less than 0.1%. Indicator cells (Raji, 1×10^6/ml) were incubated at 37 °C for 48 h in the medium (1 ml) containing *n*-butyric acid (4 mmol), TPA [20 ng (32 pmol) in DMSO 2 μl] as an inducer, and a known amount of test compound in 5 μl of DMSO. Smears were made from the cell suspension, and the activated cells stained by EBV-EA-positive serum were detected by a conventional indirect immunofluorescence technique.[46] In each assay, at least 500 cells were counted, and the number of stained cells was recorded. Triplicate assays were carried out for each compound. The average EBV-EA induction of the test compound was expressed as the relative ratio to the control experiment (100%), which was carried out with only *n*-butyric acid (4 mmol) plus TPA (32 pmol). EBV-EA induction was typically around 35%. The viability of treated Raji cells was assayed by Trypan Blue staining.

3.8. Assay for antitumor promoting activity in two-stage mouse skin carcinogenesis

Assays were performed according to a previously described method.[47,48] Specific pathogen-free female ICR mice (six weeks old) were obtained from Japan SLC Inc., Shizuoka, Japan. The animals were housed five per polycarbonate cage in a temperature-controlled room at 24±2 °C, and given water and food ad libitum throughout the experiment. The animals were divided into three groups of 15 mice each. The back of each mouse was shaved with surgical clippers one day before initiation, and the mice were topically treated with DMBA (100 μg, 390 nmol) in acetone (0.1 ml) for initiation. One week after initiation, papilloma formation was promoted by applying TPA (1 μg, 1.7 nmol) to the skin twice weekly. One hour before each TPA treatment, the mice were treated with the sample (85 nmol) in acetone (0.1 ml). The incidence of papilloma was examined weekly over 20 weeks.

Acknowledgements

The authors thank Kannonshoji Temple for kind donation of sandalwood chips used in this research. We are grateful to the SC-NMR Laboratory of Okayama University for performing the NMR spectroscopy. This study was supported in part by the U.S. National Cancer Institute, M.D. (CA17625). One of the authors (T.H.K.) acknowledges the Ministry of Education, Culture, Sports, Science and Technology of Japan for a scholarship.

References and notes

1. Kapoor, L. D. *Handbook of Ayurvedic Medicinal Plants*; CRC: Boca Raton, FL, 1990.
2. Benencia, F.; Courreges, M. C. *Phytomedicine* **1999**, *6*, 119–123.
3. Banerjee, S.; Ecavade, A.; Rao, A. R. *Cancer Lett.* **1993**, *68*, 105–109.
4. Dwivedi, C.; Abu-Ghazaleh, A. *Eur. J. Cancer Prev.* **1997**, *6*, 399–401.
5. Dwivedi, C.; Zang, Y. *Eur. J. Cancer Prev.* **1999**, *8*, 449–455.
6. Shankaranarayana, K. H.; Ayyar, K. S.; Krishna Rao, G. S. *Phytochemistry* **1980**, *19*, 1239–1240.
7. Shankaranarayana, K. H.; Ayyar, K. S.; Krishna Rao, G. S. *Curr. Sci.* **1980**, *49*, 198–199.
8. Adams, D. R.; Bhatnagar, S. P.; Cooksoon, R. C. *Phytochemistry* **1975**, *14*, 1459–1460.
9. Demole, E.; Demole, C.; Enggist, P. *Helv. Chim. Acta* **1976**, *59*, 737–747.
10. Christenson, P. A.; Secord, N.; Willis, B. J. *Phytochemistry* **1981**, *20*, 1139–1141.

11. Ranibai, P.; Ghatge, B. B.; Patil, B. B.; Bhattacharyya, S. C. *Indian J. Chem.* **1986**, *25B*, 1006–1013.
12. Gibbard, S.; Schoental, R. *J. Chromatogr.* **1969**, *44*, 396–398.
13. Okugawa, H.; Ueda, R.; Matsumoto, K.; Kawanishi, K.; Kato, A. *Phytomedicine* **1995**, *2*, 119–126.
14. Okugawa, H.; Ueda, R.; Matsumoto, K.; Kawanishi, K.; Kato, K. *Phytomedicine* **2000**, *7*, 417–422.
15. Hongratanaworakit, T.; Heuberger, E.; Buchbauer, G. *Planta Med.* **2004**, *70*, 3–7.
16. Kaur, M.; Agarwal, C.; Singh, R. P.; Guan, X.; Dwivedi, C.; Agarwal, R. *Carcinogenesis* **2005**, *26*, 369–380.
17. Dwivedi, C.; Guan, X.; Harmsen, W. L.; Voss, A. L.; Goetz-Parten, D. E.; Koopman, E. M.; Johnson, K. M.; Valluri, H. B.; Matthees, D. P. *Cancer Epidemiol. Biomarkers Prev.* **2003**, *12*, 151–156.
18. Gautschi, M.; Bajgrowicz, J. A.; Kraft, P. *Chimia* **2001**, *55*, 379–387.
19. Kim, T. H.; Ito, H.; Hayashi, K.; Hasegawa, T.; Machiguchi, T.; Yoshida, T. *Chem. Pharm. Bull.* **2005**, *53*, 641–644.
20. Kim, T. H.; Ito, H.; Hatano, T.; Hasegawa, T.; Akiba, A.; Machiguchi, T.; Yoshida, T. *J. Nat. Prod.* **2005**, *68*, 1805–1808.
21. Ochi, T.; Shibata, H.; Higuti, T.; Kodama, K.; Kusumi, T.; Takaishi, Y. *J. Nat. Prod.* **2005**, *68*, 819–824.
22. Corey, E. J.; Kirst, H. A.; Katzenellenbogen, J. A. *J. Am. Chem. Soc.* **1970**, *92*, 6314–6319.
23. Alpha, T.; Raharivelomanana, P.; Bianchini, J.-P.; Faure, R.; Cambon, A.; Joncheray, L. *Phytochemistry* **1996**, *41*, 829–831.
24. Coates, R. M.; Denissen, F. J. *J. Org. Chem.* **1998**, *53*, 2186–2192.
25. Christenson, P. A.; Willis, B. J. *J. Org. Chem.* **1979**, *44*, 2012–2018.
26. Kraut, L.; Mues, R. *Z. Naturforsch., C: Biosci.* **1999**, *54c*, 6–10.
27. Ngo, K.-S.; Brown, G. D. *Phytochemistry* **1999**, *50*, 1213–1218.
28. Hikino, H.; Suzuki, N.; Takemoto, T. *Chem. Pharm. Bull.* **1971**, *19*, 87–92.
29. Hodgson, G. L.; MacSweeney, D. F.; Money, T. *J. Chem. Soc., Perkin Trans. 1* **1973**, 2113–2130.
30. Dale, J. A.; Mosher, H. S. *J. Am. Chem. Soc.* **1973**, *95*, 512–519.
31. Ohtani, I.; Kusumi, T.; Kashman, Y.; Kakisawa, H. *J. Am. Chem. Soc.* **1991**, *113*, 4092–4096.
32. Eck, C. R.; Hodgson, G. L.; MacSweeney, D. F.; Mill, R. W.; Money, T. *J. Chem. Soc., Perkin Trans. 1* **1974**, 1938–1943.
33. Schneider, H.-J.; Weigand, E. F. *Tetrahedron* **1975**, *31*, 2125–2133.
34. Wu, T.-S.; Niwa, M.; Furukawa, H. *Phytochemistry* **1984**, *23*, 595–597.
35. Toyoda, M.; Nagashima, F.; Shima, K.; Asakawa, Y. *Phytochemistry* **1992**, *31*, 183–189.
36. Braun, N. A.; Meier, M.; Pickenhagen, W. *J. Essent. Oil Res.* **2003**, *15*, 63–65.
37. Valder, C.; Neugebauer, M.; Meier, M.; Kohlenberg, B.; Hammerschmidt, F.-J.; Braun, N. A. *J. Essent. Oil Res.* **2003**, *15*, 178–186.
38. Stermits, F. R.; Cashman, K. K.; Halligan, K. H.; Morel, C.; Tegos, G. P.; Lewis, K. *Bioorg. Med. Chem. Lett.* **2003**, *13*, 1915–1918.
39. Markham, K. R.; Geiger, H. *In the Flavonoids: Advances in Research Since 1986*; Harbone, J. B., Ed.; Chapman & Hall: London, 1994; pp 441–497.
40. Da Silva, B. P.; Bernardo, R. R.; Parente, J. P. *Phytochemistry* **2000**, *53*, 87–92.
41. Webby, F. R.; Boase, M. R. *Phytochemistry* **1999**, *52*, 939–941.
42. Bohlmann, F.; Knoll, K. H. *Phytochemistry* **1979**, *18*, 995–997.
43. Jakupovic, J.; Tan, R. X.; Bohlmann, F.; Jia, Z. J.; Huneck, S. *Planta Med.* **1991**, *57*, 450–453.
44. Miyase, T.; Kuroyanagi, M.; Noro, T.; Ueno, A.; Fukushima, S. *Chem. Pharm. Bull.* **1985**, *33*, 4445–4450.
45. Yoshizawa, S.; Horiuchi, H.; Fujiki, H.; Yoshida, T.; Okuda, T.; Sugimura, T. *Phytother. Res.* **1987**, *1*, 1190–1195.
46. Helne, G.; Helne, W. *J. Bacteriol.* **1966**, *91*, 1248–1256.
47. Ito, H.; Miyake, M.; Nishitani, E.; Mori, K.; Hatano, T.; Okuda, T.; Konoshima, T.; Takasaki, M.; Kozuka, M.; Mukainaka, T.; Tokuda, H.; Nishino, H.; Yoshida, T. *Cancer Lett.* **1999**, *143*, 5–13.
48. Ito, H.; Muranaka, T.; Mori, K.; Jin, Z.-X.; Tokuda, H.; Nishino, H.; Yoshida, T. *Chem. Pharm. Bull.* **2000**, *48*, 1720–1722.